Published in final edited form as:
Mol Cancer Res. 2014 January ; 12(1): 143–154. doi:10.1158/1541-7786.MCR-13-0184.

Integrin α3β1 Can Function to Promote Spontaneous Metastasis and Lung Colonization of Invasive Breast Carcinoma

Bo Zhou[1,#], **Katherine N. Gibson-Corley**[#2], **Mary E. Herndon**[#1], **Yihan Sun**[1,‡], **Elisabeth Gustafson-Wagner**[1,†], **Melissa Teoh-Fitzgerald**[3,¶], **Frederick E. Domann**[2,3,5], **Michael D. Henry**[2,4,5], and **Christopher S. Stipp**[1,4,5,§]

[1]Department of Biology, University of Iowa, Iowa City, IA, 52242 USA

[2]Department of Pathology, University of Iowa, Iowa City, IA, 52242 USA

[3]Free Radical and Radiation Biology Program, Department of Radiation Oncology, University of Iowa, Iowa City, IA, 52242 USA

[4]Department of Molecular Physiology & Biophysics, University of Iowa, Iowa City, IA, 52242 USA

[5]Holden Comprehensive Cancer Center, University of Iowa, Iowa City, IA, 52242 USA

[#] These authors contributed equally to this work.

Abstract

Significant evidence implicates α3β1 integrin in promoting breast cancer tumorigenesis and metastasis-associated cell behaviors in vitro and in vivo. However, the extent to which α3β1 is actually required for breast cancer metastasis remains to be determined. We used RNA interference to silence α3 integrin expression by ~70% in 4T1 murine mammary carcinoma cells, a model of aggressive, metastatic breast cancer. Loss of α3 integrin reduced adhesion, spreading, and proliferation on laminin isoforms, and modestly reduced the growth of orthotopically implanted cells. However, spontaneous metastasis to lung was strikingly curtailed. Experimental lung colonization after tail vein injection revealed a similar loss of metastatic capacity for the α3-silenced cells, suggesting that critical, α3-dependent events at the metastatic site could account for much of α3β1's contribution to metastasis in this model. Re-expressing α3 in the α3-silenced cells reversed the loss of metastatic capacity, and silencing another target, the small GTPase RhoC, had no effect, supporting the specificity of the effect of silencing α3. Parental, α3-silenced, and α3-rescued cells all secreted abundant laminin α5, an α3β1 integrin ligand, suggesting that loss of α3 integrin might disrupt an autocrine loop that could function to sustain metastatic growth. Analysis of human breast cancer cases revealed reduced survival in cases where α3 integrin and laminin-α5 are both over-expressed. Implications: α3 integrin or downstream effectors may be potential therapeutic targets in disseminated breast cancers, especially when laminin-α5 or other α3 integrin ligands are also over-expressed.

[§]To whom correspondence should be addressed: christopher-stipp@uiowa.edu.
[#]Current address: Fels Institute for Cancer Research and Molecular Biology, Temple University School of Medicine, Philadelphia, PA, USA
[‡]Current address: University of Michigan College of Pharmacy, Ann Arbor, MI, USA
[†]Current address: Integrated DNA Technologies, Coralville, IA, USA
[¶]Current address: Department of Biochemistry and Molecular Biology, University of Nebraska Medical Center, Omaha, NE, USA
bo.zhou@temple.edu; katherine-gibson-corley@uiowa.edu; mary.herndon@alum.mit.edu; yihansun@umich.edu; ewagner@idtdna.com; m.teohfitzgerald@unmc.edu; frederick-domann@uiowa.edu; michael-henry@uiowa.edu

Conflict of interest statement: the authors have no competing financial or competing non-financial interests to declare.

Keywords

α3β1 integrin; laminin-332; laminin-511; breast cancer; metastasis

Introduction

Normal mammary epithelia are surrounded by the basement membrane, an extracellular matrix rich in laminin isoforms, including laminin-332 (LM-332; LAMA3/LAMB3/LAMC2) and laminin-511 (LM-511; LAMA5/LAMB1/LAMC1). Early studies revealed that mammary carcinoma cells can co-opt LM-332 to promote anchorage independent growth and survival (1,2) and that LM-332 can potently promote breast cancer cell migration (3). Although early studies of clinical breast cancer specimens suggested that LM-332 expression is often lost during progression from ductal carcinoma in situ to invasive breast cancer (4-7), LM-332 may be retained in certain breast cancers, such as metaplastic breast carcinoma (8,9), and in a significant fraction of triple-negative, basal-like breast cancers (10). Moreover, LM-332 may be upregulated in the reactive stroma adjacent to invasive ductal carcinomas (11). In addition, compared to LM-332, LM-511 may more often be retained in advanced breast cancer (12-14), reviewed in (15). LM-511 is also abundant in adult bone marrow (16,17) and lung stroma (18) and thus may be a relevant extracellular ligand for tumor cells at metastatic sites.

Breast carcinoma cells engage laminin isoforms via integrins α3β1 (ITGA3/ITGB1) and α6β4 (ITGA6/ITGB4). Expression of β4 integrin and a coregulated gene set correlates with more a more aggressive malignant phenotype in breast cancer (19,20), and numerous functional studies have established a role for α6β4 integrin in promoting cancer cell survival, anchorage independent growth, invasion, and metastasis (reviewed in (21-23)). The tumor promoting activities of integrin α6β4 require the signaling functions of the unusually large β4 integrin cytoplasmic tail and can involve activation of RAC signaling towards NFKB (2), PI 3-kinase (PI3K) association with insulin receptor substrate-1/2 (IRS1/2) and signaling towards AKT and RAC (24,25), regulation of cAMP levels and the interplay between RHO, RAC, and protein kinase A (PRKCA) activity (26-28), stimulation of autocrine vascular endothelial growth factor (VEGF) signaling (29), crosstalk with growth factor receptors (30-32), and phosphatase SHP2 (PTPN11) signaling towards multiple downstream effectors, including the FYN tyrosine kinase (30,33,34). Some α6β4 oncogenic signaling functions may be independent of ligand binding (31), but others require ligand engagement (35).

Significant evidence also implicates integrin α3β1 as a regulator of breast cancer progression. However, the picture that has emerged of α3β1 functions in breast cancer is perhaps less clear than that of α6β4 integrin. Some early studies described an association between the loss of α3 integrin in primary breast cancer specimens and the presence of lymph node metastases (36,37). However, other studies revealed that α3β1 can contribute to breast carcinoma cell adhesion to lymph node stroma in cryostat sections (38) or to cortical bone disks, in an in vitro model of events relevant to bone metastasis (39). In one study, antibody ligation of α3 integrin on MDA-MB-231 breast carcinoma cells enhanced production of active matrix metalloproteinase-2 (MMP2), increased protrusive activity in 3D Matrigel, and increased Matrigel invasion (40). Yet a different group reported that antibody ligation of α3β1 on the same cell type impaired production of MMP9 and reduced Matrigel invasion (41). In favor of the view that α3β1 can contribute to the metastatic behavior of breast cancer cells, antibody ligation of α3β1 reduced (by ~30%) the number of MDA-MB-231 cells detected in the lungs after injection in a rat tail vein model of pulmonary arrest (42). Perhaps the strongest experimental evidence to date that α3β1 can promote

breast cancer progression in vivo comes from Mitchell et al. (43), who showed that RNAi silencing of α3 in MDA-MB-231 cells suppressed tumor growth at both subcutaneous and orthotopic sites. Thus, α3β1 integrin can play an important role in the growth of primary breast tumors; however, its role in metastatic dissemination and growth at secondary sites requires further evaluation. Moreover, our recent finding that α3β1 can act as a suppressor of metastatic colonization in a model of aggressive prostate cancer (44) underscores the need to carefully examine α3β1 in a variety of metastasis models, in order to understand the range of α3β1 functions in metastasis.

To evaluate α3β1 integrin's potential to contribute to breast cancer metastasis, we selected the 4T1 murine mammary carcinoma model. In the 4T1 model, small numbers of tumor cells implanted orthotopically in immunocompetent mice give rise to rapidly growing primary tumors that metastasize spontaneously and form macroscopic colonies in the lung and other clinically relevant sites. In addition, the 4T1 model has been reported to resemble basal-like triple-negative ductal carcinoma (45), an aggressive molecular subtype of human breast cancer. Using this model, we now provide evidence that α3β1 integrin can play a critical role in spontaneous metastasis of breast carcinoma cells by a mechanism that may involve autocrine production of the α3β1 ligand, laminin-511.

Materials and Methods

Antibodies and extracellular matrix proteins

Antibodies used in this study were rabbit anti-α3 integrin cytoplasmic tail antibody, A3-CYT (46), rabbit anti-mouse laminin α5 (47), mouse anti-myc epitope tag, (clone 9E10, Developmental Studies Hybridoma Bank), rabbit anti-RHOC (clone D40E4, Cell Signaling Inc), hamster anti-mouse α2 (ITGA2) integrin, (clone HMa2, eBioscience), rat anti-mouse α6 integrin (clone GoH3, eBioscience) and goat anti-mouse Cox-2 (PTGS2) (M19, sc-1747, Santa-Cruz Biotechnology). Alexa 488-conjugated goat-anti-rabbit, goat-anti-mouse, and goat-anti-rat secondary antibodies were purchased from Invitrogen. Cy2-conjugated goat-anti-hamster was from Jackson ImmunoResearch. Extracellular matrix proteins used in this study were laminin-332 (purified from SCC25 squamous carcinoma cell-conditioned medium as previously described (48)), rat tail collagen I (BD Bioscience), and laminin-511 (BioLamina AB).

Cell culture and RNA interference

4T1 breast carcinoma cells (ATCC) were cultured in RPMI medium. GP2-293 retroviral packaging cells (Clontech) and MDA-MB-231 cells (ATCC) were cultured in DME medium. All 4T1 and MDA-MB-231-derived cell lines were created from early passage cells that had been cultured for less than 6 months after resuscitation. Growth media were supplemented with 10% fetal bovine serum (Valley Biomedical), and 2 mM L-glutamine, 100 U/ml Penicillin, and 100 ug/ml Streptomycin (Invitrogen). EGW593.Lu cells are MDA-MB-231 cells that were recovered from a lung metastasis after orthotopic implantation of the parental cell type in the mammary fat pad of a female SCID mouse.

Retroviral particles were produced by transfection of GP2-293 cells with retroviral vectors, 0.45 μm filtering of virus-containing supernatants, and supplementing with 4 μg/ml polybrene. To facilitate monitoring tumor growth in vivo, 4T1 cells were first transduced with a luciferase cDNA in retroviral vector pQCXIN (Clontech), and selected with G418. For RNAi silencing of α3 integrin, double-stranded oligonucleotides encoding short hairpin RNAs (shRNAs) targeting the murine α3 integrin mRNA were cloned into a modified pSIREN-RetroQ retroviral vector (BD Biosciences) harboring the hygromcyin resistance maker. Transduced cells were selected with hygromycin and tested for α3 integrin

expression by cell surface labeling and immunoprecipitation with A3-CYT anti-α3 integrin antibody. We identified one effective α3 shRNA, with a targeting sequence of 5′-GTCCTATCGTCATTGCCATGA-3′. To restore α3 expression in the α3-silenced cells, we obtained a murine α3 integrin cDNA (catalog # MMM1013-9202265, source ID# 6401146, Open Biosystems) and used recombinant PCR to (i) remove the 5′ and 3′ UTRs, (ii) introduce 4 silent mutations within the shRNA targeting sequence, and (iii) add restrictions sites to facilitate cloning in frame with a 3′ Myc epitope tag in the pLXIZ retroviral vector. Stably transduced α3 rescue cells were selected with zeocin. To silence α3 integrin in human EGW593.Lu cells, shRNA constructs were prepared as described above using targeting sequences of 5′-TCACTCTGCTGGTGGACTATA-3′ (α3sh3), and '5-GGATGACTGTGAGCGG-ATGAA-3′ (α3sh4). Throughout the process of creating luciferase-labeled, α3 silenced and α3 rescue cells, all cell populations were maintained as stable, polyclonal populations to minimize concerns about clonal variation. Bioluminescence imaging of 4T1 parental, α3-silenced, and α3-rescue cells revealed all three lines had very similar luminescence of ~40 photons/sec/cell.

Cell surface labeling and flow cytometry

4T1 cells were labeled on ice with sulfo-NHS-LC-biotin (Thermo-Fisher Pierce), lysed in 1% Triton X-100 detergent (Sigma-Aldrich), and proteins were immunoprecipitated from clarified lysates, as previously described (48). Immunoprecipitates were resolved by SDS-PAGE, transfered to nitrocellulose, and visualized by blotting with IRDye-800-streptavidin (Rockland Immunochemicals, Inc) and scanning with an Odyssey infrared imaging system (LI-COR Biosciences). For flow cytometry, immunostained cells were analyzed on a Becton Dickinson FACScan flow cytometer.

Adhesion and spreading assays

For adhesion assays, wells were coated overnight with the indicated concentrations of LM-332, with 20 ug/ml collagen I, or with 10 mg/ml heat-inactivated (HI) BSA (negative control). Wells were rinsed and blocked with 10 mg/ml HI BSA. 4T1 cells were starved overnight in serum-free medium (SFM) and 20,000 cells/well were plated in SFM in each of four substrate-coated wells per condition in a 96-well plate. After 25 min at 37°C, 5% CO_2, wells were rinsed three times and adherent cells were fixed and quantified by staining with crystal violet, as previously described (48).

To assess short term cell spreading, cells were grown overnight in SFM, harvested as described above for the adhesion assay, and plated on acid-washed glass coverslips that had been coated with 1 μg/ml LM-332 or 20 μg/ml collagen I. After 30 min, cells were fixed, and photographed on a Leica DMIRE2 inverted microscope using a 20X phase objective. ImageJ software (49) was used to measure the spread area of at least 98 cells per cell type. Specific spreading was calculated by subtracting the mean area of unspread cells (fixed immediately after plating) from the spread cell areas measured at the end of the assay, as in (50).

Spontaneous metastasis assay

All animal procedures were performed according to the University of Iowa Animal Care and Use Committee policies. Female BALB/c mice (NCI-Frederick) were implanted with 5,000 cells in a volume of 50 μl in the 4^{th} mammary fat pad. Bioluminescent imaging (BLI) was performed in an IVIS100 imaging system (Caliper Life Sciences) after intraperitoneal injection of luciferin (100 μl of 15 mg/ml solution per 10 g) as described previously (51). Whole body tumor growth rates were measured as follows: a rectangular region of interest was placed around the dorsal and ventral images of each mouse, and total photon flux (photons/sec) was quantified using Living Image software v2.50 (Caliper Life Sciences).

The dorsal and ventral values were summed and mean BLI values for each group were plotted bi-weekly. Primary tumor growth was also measured by caliper, and tumor volumes were calculated using the formula $½(L \times W^2)$.

To quantify spontaneous metastasis to lung, ex-vivo BLI was performed on lungs harvested at assay endpoint (Day 31 or Day 35). To ensure the best possible uniformity of measurement conditions, mice were sacrificed in groups of 2 or 3, and lungs were immediately harvested and imaged ex-vivo. All lungs were imaged within 20-30 minutes after euthanasia. 4T1 cells colonizing the lungs were recovered by mincing the lungs with a sterile razor blade and digesting with 200 U/ml collagenase II (Worthington Biochemical Corp.) in complete medium for 15 min at 37°C. Explanted cells were grown out under G418 selection for analysis of α3 integrin expression by cell surface labeling and immunoprecipitation, as described above. Some lungs were fixed and processed for histology as described for the experimental metastasis assay, below.

Experimental metastasis assay

Female BALB/c mice were injected with 5×10^4 cells via lateral tail vein in a volume of 200 μl. Bioluminescent imaging (BLI) and quantification of whole body tumor growth rates was performed as described above for the spontaneous metastasis assay. Kaplan–Meier analysis of survival was performed using Prism 5 (GraphPad Software) on the basis that Day 0 was the day of tail vein injections and the endpoint was the day of euthanasia as determined by >10% body weight loss, hind limb paralysis or fracture, immobility, or a total photon flux $> 1 \times 10^8$, a value that initial results indicated reliably predicts death in less than one week in this model. Lungs harvested at the endpoint were fixed in 4% paraformaldehyde overnight at 4°C, rinsed, and transferred to 30% ethanol and stored at 4°C until further analysis.

For histology, lungs were routinely processed, paraffin-embedded and three 4μm thick sections were taken per lung at 300 μm intervals and stained with hematoxylin and eosin for a microscopic tumor count. Tumor counts were defined by counting tumor nodules. Tumor nodules oftentimes coalesced and were difficult to decipher. In these cases large nodules were counted as only one nodule. Three 4x fields of view were counted per slide. 3 slides per mouse were analyzed with 3 mice per group. Lungs were chosen for histology to reflect the mean value for each group as measured by BLI.

Proliferation assay

Wells were coated with 1 μg/ml LM-332, 1 μg/ml LM-511, 10 μg/ml collagen I, or left uncoated. Wells were rinsed 3 times with PBS and blocked with 5 mg/ml BSA in RPMI with 40 mM HEPES buffer pH 7.2. A total of 5,000 cells in 200 μl of RPMI plus 2% FBS was plated in 6 wells per cell type per condition in a 96 well plate. To measure cells input on day 0, an additional set of 6 wells per cell type was plated in collagen-coated wells, and assayed 2 hours later. Plates were developed by discarding 100ul from each well and adding 100 ul of solution containing RPMI with 2% FBS and WST-1 reagent (Roche Diagnostics) diluted 1:10. Plates were incubated for 1 h at 37°C and absorbance at 440 nm was measured using a plate reader.

Laminin α5 immunostaining

4T1 cells were plated on acid-washed glass coverslips coated with 10 μg/ml collagen I and cultured overnight. Cells were fixed and stained with anti-mouse laminin α5 rabbit polyclonal antiserum #8948 (generous gift of Jeffrey Miner, Washington University, St. Louis) followed by Alexa 488 goat anti-rabbit, Alexa 594 phalloidin (Invitrogen), and 0.5 μg/ml DAPI. Brightness and contrast of fluorescent images were adjusted with identical

parameters for each cell type using the Adjust > Window/Level command in ImageJ, and overlaid using the Overlay command.

Analysis of data from The Cancer Genome Atlas

The Cancer Genome Atlas (TCGA) Breast Invasive Carcinoma provisional dataset was queried using the cBioPortal interface (52,53). All tumors with mRNA data (RNA Seq V2; 914 samples as of July 2013) were tested for α3 integrin (ITGA3) over-expression (Z-score > 2) revealing over-expression in 6% of the samples. The cases affected were retrieved using the download tab and used to create a user-defined case list, which was then queried a second time for upregulation of laminin-α5 (LAMA5) mRNA (Z-score > 1), revealing upregulation in 30% of the cases. Survival data for the LAMA5 upregulated vs. LAMA5 not upregulated cases was downloaded from the interface.

Results

Stable silencing of α3 integrin in the 4T1 mammary carcinoma

To evaluate the role of α3β1 integrin in a model of spontaneous breast cancer metastasis, we used retroviral RNAi vectors to stably silence α3 integrin in 4T1 murine mammary carcinoma cells. Cell surface labeling followed by immunoprecipitation revealed a substantial reduction of α3 expression in the α3-silenced (α3si) cells compared to wild type parental cells (Fig. 1A, lanes 1 & 2). We restored α3 expression in the α3si cells by introducing a myc epitope-tagged, RNAi-resistant α3 expression vector to create α3 rescue (α3Rx) cells (Fig. 1A, lane 3). Anti-myc immunoprecipitation confirmed the expression of the α3 rescue construct in the α3Rx cells (Fig. 1A, lane 6). Quantification of several independent blots revealed that α3 expression was reduced by ~70% in the α3si cells compared to wild type, and restored to ~80% of wild type level in the α3Rx cells (Fig. 1B). The expression levels of α6 integrin, α2 integrin, and β1 integrin were not dramatically altered in the α3-silenced cells (Supplementary Table 1). Cell surface labeling followed by α6 integrin immunoprecipitation revealed that α6 pairs with the β4 subunit in 4T1 cells and confirmed that α6β4 expression was similar in all three cell types (Supplementary Fig. S1). The apparent expression level of α6β4 appeared modest compared to that of α3β1 in 4T1 parental cells. Flow cytometry of α3 itself is not possible due to lack of a suitable anti-murine α3 antibody directed at the α3 ectodomain.

Compared to wild type or α3Rx cells, the α3si cells displayed a significant reduction in adhesion on LM-332 (Fig. 1C). All three cell types adhered strongly to the α2β1 integrin ligand, collagen I and showed minimal adhesion to the BSA negative control (Fig. 1D). In short term spreading assays on LM-332, the α3si cells displayed reduced lammellipodium formation compared to wild type or α3Rx cells (compare Fig. 1F to 1E and 1G). Quantification of spread area on LM-332 revealed a reduction for the α3si cells of ~45% (Fig. 1H). Collectively, these data established that α3β1 integrin function was specifically impaired in the α3si cells and restored in the α3Rx cells.

Reduced primary tumor growth and spontaneous metastasis of α3 integrin-silenced cells

To assess the role of α3β1 integrin in breast carcinoma cells in vivo, we implanted wild type, α3si, and α3Rx cells in mammary fat pads of immunocompetent BALB/c mice. Monitoring tumor growth by bioluminescence imaging (BLI), we observed a reduced apparent tumor burden in mice harboring the α3si cells through day 10 (Fig. 2A, B, BLI color version in Supplementary Fig. S2A). At time points beyond day 10, the α3si cell tumor burden as measured by BLI was indistinguishable from wild type 4T1 cell tumor burden (Fig. 2A, B). However, caliper measurements of tumor volume revealed that α3si cell tumors were somewhat smaller than wild type or α3Rx tumors throughout the assay,

except on the final day (Fig. 2C). A potential explanation for the discrepancy between the BLI measurements and the tumor volume measurements is that large 4T1 cell tumors may display extensive areas of internal necrosis (Supplementary Fig. S3). Thus, the number of viable cells capable of contributing to the BLI signal in the larger, wild type and α3Rx tumors may constitute only a fraction of the total tumor mass, as has been reported for a bladder cancer model (54). Additional factors limiting BLI signal in large tumors may include increased optical density and reduced perfusion of poorly vascularized tumor cores with luciferin (55).

To assess spontaneous metastasis, we measured lung colonization by ex-vivo BLI at the assay endpoint. Compared to wild type or α3Rx cells, α3si 4T1 cell lung colonization was dramatically reduced, and quantification revealed an apparent ~10-fold reduction in spontaneous lung colonization by the α3si cells (Fig. 3A; BLI image in Supplementary Fig. S2B). Histologic analyses of lung colonization, both in these spontaneous metastasis assays and in experimental metastasis assays after tail vein injection, supported the results obtained from BLI measurements (See Fig. 5, below, and Supplementary Fig. S4).

In further support of the specificity of the effect of silencing α3 integrin, we established 4T1 lines harboring two separate shRNAs targeting the small GTPase, RhoC, which can promote breast cancer metastasis in other systems (56,57). Despite near total silencing of RhoC, which was maintained during in vivo passaging, these RNAi constructs had no impact on the growth of the primary tumor or on spontaneous metastasis to lung (Supplementary Fig. S5). These data indicate that neither transduction with our RNAi vector, nor instigation of active RNAi within 4T1 cells is by itself sufficient to alter their metastatic capacity. The data also indicate that RhoC appears not to be required for 4T1 cell spontaneous metastasis. The lack of impact upon silencing RhoC alone might be due to pleiotropic effects of transcription factor TWIST1 and its target miR-10b in the 4T1 cell line (58,59). Twist signaling through miR-10b can coordinately upregulate both RhoC and RhoA, among other targets, to drive breast cancer cell invasion (60).

To confirm that α3 silencing was retained in vivo over the 5 week assay, we isolated 3 sublines of each cell type from lung explants. As shown in Fig. 3B, the loss of α3 was maintained in the in vivo-derived α3si lines. Because the α3si cell primary tumors grew more slowly, especially as assessed by tumor volume, we examined the relationship between primary tumor volume and lung colonization. There was no strong relationship between the size of the primary tumor and the extent of lung colonization for any of the three cell types (Fig. 3C). Together, these data indicated that silencing α3 integrin delayed the growth of the primary tumor, especially at earlier time points, but had an even greater impact on the number of tumor cells that ultimately colonized the lung.

Dramatic reduction in experimental lung metastasis of α3 integrin-silenced cells

To begin to determine which steps in the metastatic cascade might critically depend upon α3β1, we next examined experimental lung colonization by cells injected via tail vein. BLI immediately post-injection confirmed that cells arrested in the lungs (Fig. 4A, BLI color version in Supplementary Fig. S2C). Two weeks post-injection, BLI revealed a dramatic reduction in lung colonization by α3si cells compared to wild type or α3Rx cells (Fig. 4A). Quantification of BLI images confirmed that α3si cell colonization was significantly impaired from day 12 onward, with over an order of magnitude reduction in apparent tumor burden evident by day 18 (Fig. 4B). In addition, survival of mice bearing α3si tumor cells was significantly enhanced compared to mice bearing wild type or α3Rx cells (Fig. 4C). In both the BLI and survival analyses, the α3Rx cells displayed an intermediate phenotype at some time points, suggesting that α3 function may not be completely rescued in the α3Rx cells with regards to experimental lung colonization.

To confirm the results of the BLI analysis, we also performed gross and histologic analysis of lungs recovered at the endpoint of the assay. Compared to lungs from mice harboring wild type or α3Rx 4T1 cells, far fewer metastatic nodules were grossly evident on the surface of lungs harboring α3si 4T1 cells (Fig. 5A). Quantification of tumor nodules in hematoxylin-eosin (H&E)-stained sections confirmed that α3si cells formed significantly fewer nodules than either wild type or α3Rx cells (Fig. 5B-E). Again, the α3Rx cells displayed an intermediate phenotype, consistent with the BLI data. We also performed a histologic analysis of archived lungs of mice from the spontaneous metastasis assay in Figs. 2 and 3. Although the data were more highly variable due to the fact that fewer intact lungs were available, the histologic results were in agreement with the BLI analysis, with α3si 4T1 cells forming many fewer tumor nodules (Supplementary Fig. S4). An interesting feature noted in Fig. S4 (inset) is the large number of neutrophils throughout the pulmonary vasculature in these mice by the end of the spontaneous metastasis assay, consistent with an earlier report (61). The large number of intravascular neutrophils present suggests that regulation of tumor cell-neutrophil interactions may be a factor to consider in future studies of α3 integrin function in the 4T1 metastasis model. In sum, these data revealed that, whatever its contribution to early invasive events at the primary site, α3β1 integrin is also likely to strongly influence the ability of breast carcinoma cells to colonize the lung once they have disseminated from the primary tumor.

α3β1-silenced 4T1 cells display diminished proliferation on laminin isoforms and secrete LM-511, an endogenous α3β1 ligand

Integrin α3β1 may promote pro-metastatic breast cancer cell behaviors via multiple downstream pathways including regulation of cyclooxygenase (COX)-2, (VEGF) secretion, and MMP production (62). However, we were unable to detect significant differences in COX-2, VEGF, or MMP production in our 4T1 cell lines (Supplementary Fig. S6A-C). Transendothelial migration assays of our 4T1 cell lines suggested a modest decrease in migration for the α3si cells, but the effect did not reach statistical significance (Fig. S6D). In short term proliferation assays, the α3si cells displayed reduced proliferation not only on LM-332 and LM-511, but also on collagen I or uncoated plastic (Fig. 6). The reduced proliferation of the α3si cells irrespective of the exogenous ligand supplied suggested the possibility that an endogenous α3 integrin ligand may be contributing to proliferation in our assay.

Pouliot and colleagues have reported that a bone-metastatic subclone of 4T1 cells expresses LM-511, which may be an important regulator of metastastic colonization in this system (14,63,64). Immunostaining cultures of our wild type, α3si, and α3Rx cells for LM-511 revealed that all three of our 4T1 cell lines also secrete abundant LM-511, some of which seems to be cell-associated (Fig. 7A-F), and some of which is deposited on the substrate (Fig. 7G-I). LM-511 secretion was not overtly affected by the loss of α3β1 integrin; however, these data confirmed that 4T1 cells produce an autocrine extracellular ligand with the potential to promote growth and survival via α3β1 integrin-dependent signaling.

To further explore the relationship between laminin secretion and α3β1-dependent proliferation, we silenced α3 integrin in EGW593.lu cells, an in vivo-passaged subline of MDA-MB-231 breast carcinoma cells, which fail to secrete detectable LM-511 or LM-332 (Supplementary Fig. S7A). Despite achieving silencing comparable to or superior to that which we achieved in 4T1 cells, no obvious differences were observed in short term proliferation assays comparing the control and α3-silenced MDA-MB-231 cell lines (Fig. S7B). Collectively, these data suggested that the role of α3β1 in breast carcinoma may depend on whether an α3β1 ligand is co-expressed by the carcinoma cells.

To begin to test the relevance of our findings to human cancers, we queried the Cancer Genome Atlas (TCGA) database. Integrin α3 was upregulated (Z-score > +2) in 6% of the samples in the Breast Invasive Carcinoma/TCGA Provisional dataset. Among patients with upregulated α3 integrin, those with tumors in which laminin-α5 (LAMA5) was also upregulated (Z-score > +1) had significantly worse overall survival than those with tumors in which LAMA5 was not upregulated (median survival time 51 months vs. 114 months; Fig. 7M). When examined separately, changes in mRNA expression of α3 integrin or LAMA5 were not on their own linked to significant survival differences. The decreased survival was specifically linked to cases in which both α3 integrin and LAMA5 were upregulated.

Discussion

Integrin α3β1 can function to promote breast cancer metastasis in vivo

The ability to evaluate the role of α3 integrin in breast cancer metastasis had been complicated by the perinatal-lethal phenotype of α3 knock-out mice (65). Studies with conditional α3 knock out mice, which were only created relatively recently, have thus far demonstrated critical roles for α3 integrin in skin tumor formation (66), regulation of mammary myoepithelial cell contractility (67) and control of wound healing rate (68); however, studies examining the effect of α3 deletion in breast cancer models have not yet been reported. Antibody blockade of α3 can reduce MDA-MB-231 pulmonary arrest (42) and suppress metastatic colonization of several tumor types upon tail vein, intracardiac, intracerebral, or peritoneal injection (reviewed in (69)). However, anti-α3 antibodies have had disparate effects on tumor cell behaviors in vitro (40,41), which could raise questions about the precise mechanism of antibody action in vivo. Silencing α3 in MDA-MB-231 cells suppressed the growth of tumors implanted both subcutaneously and in mammary fat pad (43), revealing a role for α3 in promoting the growth of breast cancer cells at the primary site, but leaving open the question of the role of α3 in metastasis.

Our new data using the 4T1 cell model now establish that loss of α3 integrin expression can cause a substantial reduction in breast cancer metastatic capacity in vivo. The α3-silenced 4T1 cell tumors grew somewhat more slowly at the primary site, but (i) the reduction of the apparent metastatic tumor burden of the α3-silenced cells was striking compared to the modest reduction in their growth at the primary site, and (ii) analysis of primary tumor size versus lung metastasis did not reveal a correlation, suggesting that the modestly reduced growth at the primary site is not sufficient to explain the dramatic reduction in lung metastasis. Our data do not rule out a contribution by α3β1 to early events in the metastatic cascade, but experimental lung colonization of α3-silenced tumor cells after tail vein injection was reduced to a similar extent as spontaneous metastasis after fat pad injection. This result suggests that inhibition of critical, α3-dependent events at the metastatic site may be sufficient to account for much of the reduction in the spontaneous metastasis of α3-silenced cells from the fat pad.

Potential mechanisms for α3β1 integrin contributions to breast cancer metastasis

The contributions of α3β1 integrin to events at the metastatic site could include pulmonary arrest, extravasation, and proliferation to form macroscopic metastases. A recent study demonstrated that 4T1 cells selected for enhanced chemotaxis to LM-511 in vitro displayed increased spontaneous metastasis to bone in vivo, and a snake venom disintegrin that inhibits α3, α6, and α7 integrins, inhibited 4T1 cell migration and invasion towards LM-511 (64). LM-511 is also widely expressed in endothelial cell basement membranes of the arteries, veins, and capillaries of lung, brain and lymph nodes (70), and may thus be an important extracellular ligand for tumor cells during extravasation. We observed a moderate

but significant reduction in α3β1-dependent adhesion and spreading in our α3-silenced cells. We also observed reduced proliferation, not only on laminin isoforms, but also on collagen I or on uncoated plastic. This prompted us to examine autocrine production of the α3β1 integrin ligand, LM-511. As previously reported for a bone-metastatic 4T1 cell subclone (14), our 4T1 cells also secrete abundant LM-511. Thus, autocrine LM-511 may promote 4T1 cell survival and proliferation at the metastatic site, and loss of α3 integrin may partially disrupt this autocrine proliferation pathway. In support of this possibility, silencing α3 integrin in MDA-MB-231-derived EGW593.lu breast carcinoma cells, which fail to secrete LM-511, did not affect short-term proliferation, suggesting that these cells do not depend on such an autocrine loop. The contributions of α3β1 to MDA-MB-231 tumor growth in vivo may instead involve tumor cell crosstalk to endothelial cells via an α3β1-controlled COX-2-dependent mechanism (43). Compared to 4T1 cells, metastasis of MDA-MB-231 cells occurs with slower kinetics and fewer metastatic colonies, even though immunocompromised hosts must be used. This suggests that co-expression of both α3β1 and an α3β1 ligand in breast carcinoma may contribute to a more aggressive, metastatic phenotype, a possibility that is supported by our analysis of data from the Breast Invasive Carcinoma TCGA database. The signaling effectors downstream of α3β1 that support metastasis remain to be defined, but could include focal adhesion kinase (PTK2), MAPK, or Rac1-dependent pathways (71-73).

Partial loss of α3 function in vitro can produce large impacts on metastasis in vivo – a potential therapeutic window for α3 integrin antagonists?

Compared to the reductions in spontaneous and experimental metastasis that we observed for α3-silenced 4T1 cells in vivo, the in vitro phenotypes of the α3-silenced cells were more modest. It is certainly possible that we have not yet identified an in vitro assay that captures the critical function for α3 in 4T1 cell metastasis in vivo, but another potential explanation for this apparent discrepancy could be that there are multiple, α3-dependent steps in the metastatic cascade. If 3 or 4 steps in metastasis depend strongly on α3 function, a 40% reduction in α3 function could result in an ~80-90% reduction in metastatic efficiency due to synergistic effects ($0.6^3 = 0.22$, $0.6^4 = 0.13$). In a scenario where α3 functions mainly in proliferation at the metastatic site, it is of interest to note that, in order for a single cell to produce a macroscopic metastatic colony of ~1×10^6 cells, ~21 cell doublings are required. A reduction in proliferation efficiency of only ~10% per doubling would then result in around 90% reduction in colony size after 21 doublings ($0.9^{21} = 0.11$). These mathematical considerations suggest that even a modest reduction in α3 function in breast cancer cells could have a dramatic impact on metastatic efficiency. For tumor cells that overexpress α3 integrin and critically depend on α3 for metastatic colonization, there may then be a therapeutic window wherein interfering with α3 function could significantly curtail metastasis without severely compromising α3 function in normal tissues. The ability of a high affinity, α3 integrin-binding cyclic peptide to selectively target α3 overexpressing tumor cells in vivo (74,75) supports the notion that α3 antagonists might have the potential to specifically target tumor cells while leaving α3 function in normal tissues relatively intact.

In conclusion, our new data now establish that α3 integrin can make critical contributions to breast cancer metastasis in vivo. Seemingly modest reductions in α3 function, as measured in in vitro assays can have a substantial impact on metastatic behavior in vivo. This could reflect α3 function at multiple levels of the metastatic cascade or an ongoing requirement for α3 in proliferation at the metastatic site, potentially through an autocrine mechanism in which breast cancer cells take advantage of constitutive secretion of an α3 integrin ligand, such as LM-511. Future pre-clinical experiments should aim to explore (i) whether α3 antagonists may have utility as adjuvant therapeutics in combination other strategies to

curtail the growth of metastatic α3β1-positive breast cancers, and (ii) the relationship between the co-expression of α3β1 and its ligands and breast cancer metastatic behavior.

Supplementary Material

Refer to Web version on PubMed Central for supplementary material.

Acknowledgments

Flow cytometry data presented herein were obtained at the Flow Cytometry Facility, which is a Carver College of Medicine Core Research Facilities/ Holden Comprehensive Cancer Center Core Laboratory at the University of Iowa. Anti-laminin α5 antibody was generously provided by Jeffrey Miner, Washington University School of Medicine.

Grant Support

This work was supported by NIH R01 CA136664 and a seed grant from the University of Iowa Holden Comprehensive Cancer Center Breast Cancer Research Interest Group (C.S.S.), NIH R01 CA115438 (F.E.D.), and NIH R01 CA130916 (M.D.H.).

References

1. Weaver VM, Lelièvre S, Lakins JN, Chrenek MA, Jones JCR, Giancotti F, et al. beta4 integrin-dependent formation of polarized three-dimensional architecture confers resistance to apoptosis in normal and malignant mammary epithelium. Cancer Cell. 2002; 2:205–16. [PubMed: 12242153]
2. Zahir N, Lakins JN, Russell A, Ming W, Chatterjee C, Rozenberg GI, et al. Autocrine laminin-5 ligates alpha6beta4 integrin and activates RAC and NFkappaB to mediate anchorage-independent survival of mammary tumors. J Cell Biol. 2003; 163:1397–407. [PubMed: 14691145]
3. Plopper GE, Domanico SZ, Cirulli V, Kiosses WB, Quaranta V. Migration of breast epithelial cells on Laminin-5: differential role of integrins in normal and transformed cell types. Breast Cancer Res Treat. 1998; 51:57–69. [PubMed: 9877029]
4. Martin KJ, Kwan CP, Nagasaki K, Zhang X, O'Hare MJ, Kaelin CM, et al. Down-regulation of laminin-5 in breast carcinoma cells. Mol Med. 1998; 4:602–13. [PubMed: 9848077]
5. Henning K, Berndt A, Katenkamp D, Kosmehl H. Loss of laminin-5 in the epithelium-stroma interface: an immunohistochemical marker of malignancy in epithelial lesions of the breast. Histopathology. 1999; 34:305–9. [PubMed: 10231397]
6. Sathyanarayana UG, Padar A, Huang CX, Suzuki M, Shigematsu H, Bekele BN, et al. Aberrant promoter methylation and silencing of laminin-5-encoding genes in breast carcinoma. Clin Cancer Res. 2003; 9:6389–94. [PubMed: 14695139]
7. Korah R, Das K, Lindy ME, Hameed M, Wieder R. Coordinate loss of fibroblast growth factor 2 and laminin 5 expression during neoplastic progression of mammary duct epithelium. Hum Pathol. 2007; 38:154–60. [PubMed: 16996573]
8. Carpenter PM, Wang-Rodriguez J, Chan OTM, Wilczynski SP. Laminin 5 expression in metaplastic breast carcinomas. Am J Surg Pathol. 2008; 32:345–53. [PubMed: 18300817]
9. Carpenter PM, Dao AV, Arain ZS, Chang MK, Nguyen HP, Arain S, et al. Motility induction in breast carcinoma by mammary epithelial laminin 332 (laminin 5). Mol Cancer Res. 2009; 7:462–75. [PubMed: 19351903]
10. Kwon S-Y, Chae SW, Wilczynski SP, Arain A, Carpenter Philip M. Laminin 332 expression in breast carcinoma. Appl Immunohistochem Mol Morphol. 2012; 20:159–64. [PubMed: 22427740]
11. Kim BG, An HJ, Kang S, Choi YP, Gao M-Q, Park H, et al. Laminin-332-rich tumor microenvironment for tumor invasion in the interface zone of breast cancer. Am J Pathol. 2011; 178:373–81. [PubMed: 21224074]
12. Hewitt RE, Powe DG, Morrell K, Balley E, Leach IH, Ellis IO, et al. Laminin and collagen IV subunit distribution in normal and neoplastic tissues of colorectum and breast. Br J Cancer. 1997; 75:221–9. [PubMed: 9010030]

13. Määttä M, Virtanen I, Burgeson R, Autio-Harmainen H. Comparative analysis of the distribution of laminin chains in the basement membranes in some malignant epithelial tumors: the alpha1 chain of laminin shows a selected expression pattern in human carcinomas. J. Histochem. Cytochem. 2001; 49:711–26. [PubMed: 11373318]
14. Chia J, Kusuma N, Anderson R, Parker B, Bidwell B, Zamurs L, et al. Evidence for a role of tumor-derived laminin-511 in the metastatic progression of breast cancer. Am J Pathol. 2007; 170:2135–48. [PubMed: 17525279]
15. Pouliot N, Kusuma N. Laminin-511: a multi-functional adhesion protein regulating cell migration, tumor invasion and metastasis. Cell Adh Migr. 2013; 7:142–9. [PubMed: 23076212]
16. Siler U, Seiffert M, Puch S, Richards A, Torok-Storb B, Müller CA, et al. Characterization and functional analysis of laminin isoforms in human bone marrow. Blood. 2000; 96:4194–203. [PubMed: 11110691]
17. Gu Y, Sorokin L, Durbeej M, Hjalt T, Jönsson JI, Ekblom M. Characterization of bone marrow laminins and identification of alpha5-containing laminins as adhesive proteins for multipotent hematopoietic FDCP-Mix cells. Blood. 1999; 93:2533–42. [PubMed: 10194432]
18. Pierce RA, Griffin GL, Miner JH, Senior RM. Expression patterns of laminin alpha1 and alpha5 in human lung during development. Am. J. Respir. Cell Mol. Biol. 2000; 23:742–7. [PubMed: 11104726]
19. Diaz LK, Cristofanilli M, Zhou X, Welch KL, Smith TL, Yang Y, et al. Beta4 integrin subunit gene expression correlates with tumor size and nuclear grade in early breast cancer. Mod Pathol. 2005; 18:1165–75. [PubMed: 15920552]
20. Lu S, Simin K, Khan A, Mercurio AM. Analysis of integrin beta4 expression in human breast cancer: association with basal-like tumors and prognostic significance. Clin Cancer Res. 2008; 14:1050–8. [PubMed: 18281537]
21. Lipscomb EA, Mercurio AM. Mobilization and activation of a signaling competent alpha6beta4integrin underlies its contribution to carcinoma progression. Cancer Metastasis Rev. 2005; 24:413–23. [PubMed: 16258729]
22. Wilhelmsen K, Litjens SHM, Sonnenberg A. Multiple functions of the integrin alpha6beta4 in epidermal homeostasis and tumorigenesis. Mol Cell Biol. 2006; 26:2877–86. [PubMed: 16581764]
23. Giancotti FG. Targeting integrin beta4 for cancer and anti-angiogenic therapy. Trends Pharmacol. Sci. 2007; 28:506–11. [PubMed: 17822782]
24. Shaw LM, Rabinovitz I, Wang HH, Toker A, Mercurio AM. Activation of phosphoinositide 3-OH kinase by the alpha6beta4 integrin promotes carcinoma invasion. Cell. 1997; 91:949–60. [PubMed: 9428518]
25. Shaw LM. Identification of insulin receptor substrate 1 (IRS-1) and IRS-2 as signaling intermediates in the alpha6beta4 integrin-dependent activation of phosphoinositide 3-OH kinase and promotion of invasion. Mol Cell Biol. 2001; 21:5082–93. [PubMed: 11438664]
26. O'Connor KL, Shaw LM, Mercurio AM. Release of cAMP gating by the alpha6beta4 integrin stimulates lamellae formation and the chemotactic migration of invasive carcinoma cells. J Cell Biol. 1998; 143:1749–60. [PubMed: 9852165]
27. O'Connor KL, Nguyen BK, Mercurio AM. RhoA function in lamellae formation and migration is regulated by the alpha6beta4 integrin and cAMP metabolism. J Cell Biol. 2000; 148:253–8. [PubMed: 10648558]
28. O'Connor KL, Chen M, Towers LN. Integrin α6β4 cooperates with LPA signaling to stimulate Rac through AKAP-Lbc-mediated RhoA activation. Am. J. Physiol., Cell Physiol. 2012; 302:C605–14. [PubMed: 22049212]
29. Chung J, Bachelder RE, Lipscomb EA, Shaw LM, Mercurio AM. Integrin (alpha 6 beta 4) regulation of eIF-4E activity and VEGF translation: a survival mechanism for carcinoma cells. J Cell Biol. 2002; 158:165–74. [PubMed: 12105188]
30. Bertotti A, Comoglio PM, Trusolino L. Beta4 integrin activates a Shp2-Src signaling pathway that sustains HGF-induced anchorage-independent growth. J Cell Biol. 2006; 175:993–1003. [PubMed: 17158954]
31. Bertotti A, Comoglio PM, Trusolino L. Beta4 integrin is a transforming molecule that unleashes Met tyrosine kinase tumorigenesis. Cancer Res. 2005; 65:10674–9. [PubMed: 16322210]

32. Guo W, Pylayeva Y, Pepe A, Yoshioka T, Muller WJ, Inghirami G, et al. Beta 4 integrin amplifies ErbB2 signaling to promote mammary tumorigenesis. Cell. 2006; 126:489–502. [PubMed: 16901783]
33. Dutta U, Shaw LM. A key tyrosine (Y1494) in the beta4 integrin regulates multiple signaling pathways important for tumor development and progression. Cancer Res. 2008; 68:8779–87. [PubMed: 18974120]
34. Yang X, Dutta U, Shaw LM. SHP2 mediates the localized activation of Fyn downstream of the α6β4 integrin to promote carcinoma invasion. Mol Cell Biol. 2010; 30:5306–17. [PubMed: 20855525]
35. Merdek KD, Yang X, Taglienti CA, Shaw LM, Mercurio AM. Intrinsic signaling functions of the beta4 integrin intracellular domain. J Biol Chem. 2007; 282:30322–30. [PubMed: 17711859]
36. Gui GP, Wells CA, Yeomans P, Jordan SE, Vinson GP, Carpenter R. Integrin expression in breast cancer cytology: a novel predictor of axillary metastasis. Eur J Surg Oncol. 1996; 22:254–8. [PubMed: 8654607]
37. Gui GP, Wells CA, Browne PD, Yeomans P, Jordan S, Puddefoot JR, et al. Integrin expression in primary breast cancer and its relation to axillary nodal status. Surgery. 1995; 117:102–8. [PubMed: 7809822]
38. Tawil NJ, Gowri V, Djoneidi M, Nip J, Carbonetto S, Brodt P. Integrin alpha3beta1 can promote adhesion and spreading of metastatic breast carcinoma cells on the lymph node stroma. Int J Cancer. 1996; 66:703–10. [PubMed: 8647636]
39. Lundström A, Holmbom J, Lindqvist C, Nordström T. The role of alpha2 beta1 and alpha3 beta1 integrin receptors in the initial anchoring of MDA-MB-231 human breast cancer cells to cortical bone matrix. Biochem Biophys Res Commun. 1998; 250:735–40. [PubMed: 9784415]
40. Sugiura T, Berditchevski F. Function of alpha3beta1-tetraspanin protein complexes in tumor cell invasion. Evidence for the role of the complexes in production of matrix metalloproteinase 2 (MMP-2). J Cell Biol. 1999; 146:1375–89. [PubMed: 10491398]
41. Morini M, Mottolese M, Ferrari N, Ghiorzo F, Buglioni S, Mortarini R, et al. The alpha 3 beta 1 integrin is associated with mammary carcinoma cell metastasis, invasion, and gelatinase B (MMP-9) activity. Int J Cancer. 2000; 87:336–42. [PubMed: 10897037]
42. Wang H, Fu W, Im JH, Zhou Z, Santoro SA, Iyer V, et al. Tumor cell alpha3beta1 integrin and vascular laminin-5 mediate pulmonary arrest and metastasis. J Cell Biol. 2004; 164:935–41. [PubMed: 15024036]
43. Mitchell K, Svenson KB, Longmate WM, Gkirtzimanaki K, Sadej R, Wang X, et al. Suppression of integrin alpha3beta1 in breast cancer cells reduces cyclooxygenase-2 gene expression and inhibits tumorigenesis, invasion, and cross-talk to endothelial cells. Cancer Res. 2010; 70:6359–67. [PubMed: 20631072]
44. Varzavand A, Drake JM, Svensson RU, Herndon ME, Zhou B, Henry MD, et al. Integrin α3β1 regulates tumor cell responses to stromal cells and can function to suppress prostate cancer metastatic colonization. Clin Exp Metastasis. 2012
45. Bao L, Haque A, Jackson K, Hazari S, Moroz K, Jetly R, et al. Increased expression of P-glycoprotein is associated with doxorubicin chemoresistance in the metastatic 4T1 breast cancer model. Am J Pathol. 2011; 178:838–52. [PubMed: 21281816]
46. Zevian S, Winterwood NE, Stipp CS. Structure-function analysis of tetraspanin CD151 reveals distinct requirements for tumor cell behaviors mediated by α3β1 versus α6β4 integrin. Journal of Biological Chemistry. 2011; 286:7496–506. [PubMed: 21193415]
47. Miner JH, Patton BL, Lentz SI, Gilbert DJ, Snider WD, Jenkins NA, et al. The laminin alpha chains: expression, developmental transitions, and chromosomal locations of alpha1-5, identification of heterotrimeric laminins 8-11, and cloning of a novel alpha3 isoform. J Cell Biol. 1997; 137:685–701. [PubMed: 9151674]
48. Winterwood NE, Varzavand A, Meland MN, Ashman LK, Stipp CS. A critical role for tetraspanin CD151 in alpha3beta1 and alpha6beta4 integrin-dependent tumor cell functions on laminin-5. Mol Biol Cell. 2006; 17:2707–21. [PubMed: 16571677]
49. Schneider CA, Rasband WS, Eliceiri KW. NIH Image to ImageJ: 25 years of image analysis. Nat Methods. 2012; 9:671–5. [PubMed: 22930834]

50. Stipp CS, Kolesnikova TV, Hemler ME. EWI-2 regulates alpha3beta1 integrin-dependent cell functions on laminin-5. J Cell Biol. 2003; 163:1167–77. [PubMed: 14662754]
51. Drake JM, Gabriel CL, Henry MD. Assessing tumor growth and distribution in a model of prostate cancer metastasis using bioluminescence imaging. Clin Exp Metastasis. 2005; 22:674–84. [PubMed: 16703413]
52. Cerami E, Gao J, Dogrusoz U, Gross BE, Sumer SO, Aksoy BA, et al. The cBio cancer genomics portal: an open platform for exploring multidimensional cancer genomics data. Cancer Discov. 2012; 2:401–4. [PubMed: 22588877]
53. Gao J, Aksoy BA, Dogrusoz U, Dresdner G, Gross B, Sumer SO, et al. Integrative analysis of complex cancer genomics and clinical profiles using the cBioPortal. Sci Signal. 2013; 6:pl1. [PubMed: 23550210]
54. Black PC, Shetty A, Brown GA, Esparza-Coss E, Metwalli AR, Agarwal PK, et al. Validating bladder cancer xenograft bioluminescence with magnetic resonance imaging: the significance of hypoxia and necrosis. BJU Int. 2010; 106:1799–804. [PubMed: 20500508]
55. Hilali El N, Rubio N, Martinez-Villacampa M, Blanco J. Combined noninvasive imaging and luminometric quantification of luciferase-labeled human prostate tumors and metastases. Lab Invest. 2002; 82:1563–71. [PubMed: 12429816]
56. Hakem A, Sanchez-Sweatman O, You-Ten A, Duncan G, Wakeham A, Khokha R, et al. RhoC is dispensable for embryogenesis and tumor initiation but essential for metastasis. Genes Dev. 2005; 19:1974–9. [PubMed: 16107613]
57. Rosenthal DT, Zhang J, Bao L, Zhu L, Wu Z, Toy K, et al. RhoC impacts the metastatic potential and abundance of breast cancer stem cells. PLoS ONE. 2012; 7:e40979. [PubMed: 22911725]
58. Yang J, Mani SA, Donaher JL, Ramaswamy S, Itzykson RA, Come C, et al. Twist, a master regulator of morphogenesis, plays an essential role in tumor metastasis. Cell. 2004; 117:927–39. [PubMed: 15210113]
59. Ma L, Reinhardt F, Pan E, Soutschek J, Bhat B, Marcusson EG, et al. Therapeutic silencing of miR-10b inhibits metastasis in a mouse mammary tumor model. Nat Biotechnol. 2010; 28:341–7. [PubMed: 20351690]
60. Bourguignon LYW, Wong G, Earle C, Krueger K, Spevak CC. Hyaluronan-CD44 interaction promotes c-Src-mediated twist signaling, microRNA-10b expression, and RhoA/RhoC up-regulation, leading to Rho-kinase-associated cytoskeleton activation and breast tumor cell invasion. Journal of Biological Chemistry. 2010; 285:36721–35. [PubMed: 20843787]
61. Granot Z, Henke E, Comen EA, King TA, Norton L, Benezra R. Tumor entrained neutrophils inhibit seeding in the premetastatic lung. Cancer Cell. 2011; 20:300–14. [PubMed: 21907922]
62. Subbaram, S.; Dipersio, CM. Expert Opin. Ther. Targets. Vol. 15. Informa UK, Ltd; London: 2011. Integrin α3β1 as a breast cancer target; p. 1197-210.
63. Kusuma N, Anderson RL, Pouliot N. Laminin α5-derived peptides modulate the properties of metastatic breast tumour cells. Clin Exp Metastasis. 2011; 28:909–21. [PubMed: 21938437]
64. Kusuma N, Denoyer D, Eble JA, Redvers RP, Parker BS, Pelzer R, et al. Integrin-dependent response to laminin-511 regulates breast tumor cell invasion and metastasis. Int J Cancer. 2012; 130:555–66. [PubMed: 21387294]
65. Kreidberg JA, Donovan MJ, Goldstein SL, Rennke H, Shepherd K, Jones RC, et al. Alpha 3 beta 1 integrin has a crucial role in kidney and lung organogenesis. Development. 1996; 122:3537–47. [PubMed: 8951069]
66. Sachs N, Secades P, van Hulst L, Kreft M, Song J-Y, Sonnenberg A. Loss of integrin α3 prevents skin tumor formation by promoting epidermal turnover and depletion of slow-cycling cells. Proc Natl Acad Sci USA. 2012; 109:21468–73. [PubMed: 23236172]
67. Raymond K, Cagnet S, Kreft M, Janssen H, Sonnenberg A, Glukhova MA. Control of mammary myoepithelial cell contractile function by α3β1 integrin signalling. EMBO J. 2011; 30:1896–906. [PubMed: 21487391]
68. Margadant C, Raymond K, Kreft M, Sachs N, Janssen H, Sonnenberg A. Integrin {alpha}3{beta}1 inhibits directional migration and wound re-epithelialization in the skin. J Cell Sci. 2009; 122:278–88. [PubMed: 19118220]

69. Stipp CS. Laminin-binding integrins and their tetraspanin partners as potential antimetastatic targets. Expert Rev Mol Med. 2010; 12:e3. [PubMed: 20078909]

70. Sorokin LM, Pausch F, Frieser M, Kröger S, Ohage E, Deutzmann R. Developmental regulation of the laminin alpha5 chain suggests a role in epithelial and endothelial cell maturation. Dev Biol. 1997; 189:285–300. [PubMed: 9299121]

71. Manohar A, Shome SG, Lamar J, Stirling L, Iyer V, Pumiglia K, et al. Alpha 3 beta 1 integrin promotes keratinocyte cell survival through activation of a MEK/ERK signaling pathway. J Cell Sci. 2004; 117:4043–54. [PubMed: 15280429]

72. Choma DP, Pumiglia K, Dipersio CM. Integrin alpha3beta1 directs the stabilization of a polarized lamellipodium in epithelial cells through activation of Rac1. J Cell Sci. 2004; 117:3947–59. [PubMed: 15265981]

73. Choma DP, Milano V, Pumiglia KM, Dipersio CM. Integrin alpha3beta1-dependent activation of FAK/Src regulates Rac1-mediated keratinocyte polarization on laminin-5. J Invest Dermatol. 2007; 127:31–40. [PubMed: 16917494]

74. Aina OH, Liu R, Sutcliffe JL, Marik J, Pan C-X, Lam KS. From combinatorial chemistry to cancer-targeting peptides. Mol Pharm. 2007; 4:631–51. [PubMed: 17880166]

75. Xiao K, Li Y, Lee JS, Gonik AM, Dong T, Fung G, et al. “OA02” peptide facilitates the precise targeting of paclitaxel-loaded micellar nanoparticles to ovarian cancer in vivo. Cancer Res. 2012; 72:2100–10. [PubMed: 22396491]

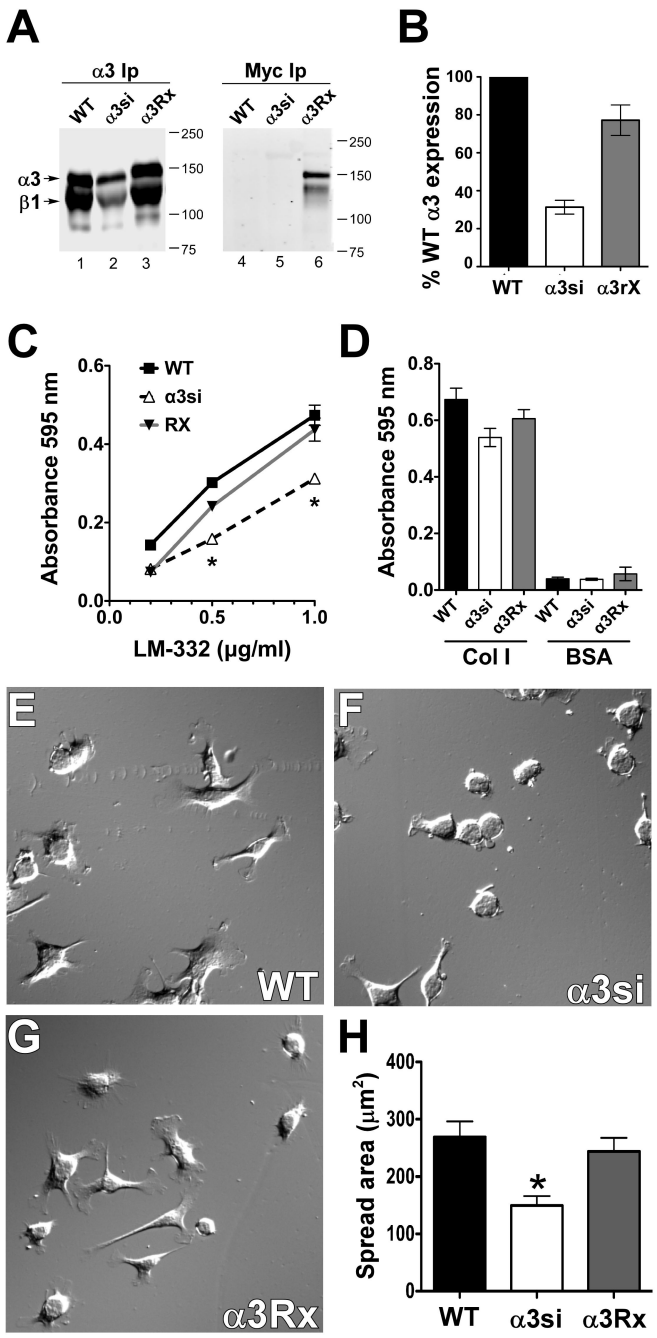

Figure 1. Impaired adhesion and spreading of α3 integrin-silenced 4T1 carcinoma cells

(**A**) Cell surface biotinylated wild type (WT), α3-silenced (α3si), and α3-rescued (α3Rx) 4T1 cells were lysed in 1% Triton X-100 detergent and α3β1 integrin was immunoprecipitated using the A3-CYT polyconal antibody (lanes 1-3) or the 9E10 anti-myc epitope antibody (lanes 4-6). The blot was visualized with DyLight 800-Neutravidin. Arrows indicate the α3 and β1 integrin bands. (**B**) Quantification of multiple independent blots by LI-COR infrared fluorescent scanner. Data are presented as % wild type expression ± SEM, n=6 blots. (**C**) Wild type, α3si, and α3Rx 4T1 cells were plated in wells with different coating concentrations of LM-332. After 25 min, non-adherent cells were removed by rinsing, and adherent cells were quantified by crystal violet staining. Compared to wild

type or α3Rx cells, the α3si cells showed significantly reduced adhesion on wells coated 0.5 μg/ml and 1.0 μg/ml LM-332 (*P<0.001, ANOVA with Tukey post-test, n=4 wells/condition). (**D**) Wild type, α3si, and α3Rx 4T1 cells were plated on wells coated with 20 μg/ml collagen I or in BSA-blocked negative control wells. After 25 min, adherent cells were quantified as in (A). (**E-G**) Wild type, α3si, and α3Rx 4T1 cells were plated on glass coverslips coated with 1 μg/ml LM-332 for 30 min and then fixed and photographed with differential interference microscopy. (**H**) The spread area of wild type, α3si, and α3Rx cells was quantified with ImageJ software, as described in Materials and Methods. The spread area of α3si cells was significantly less than wild type or α3Rx cells (*P<0.01, ANOVA with Tukey post test, n≥98 cells per cell type).

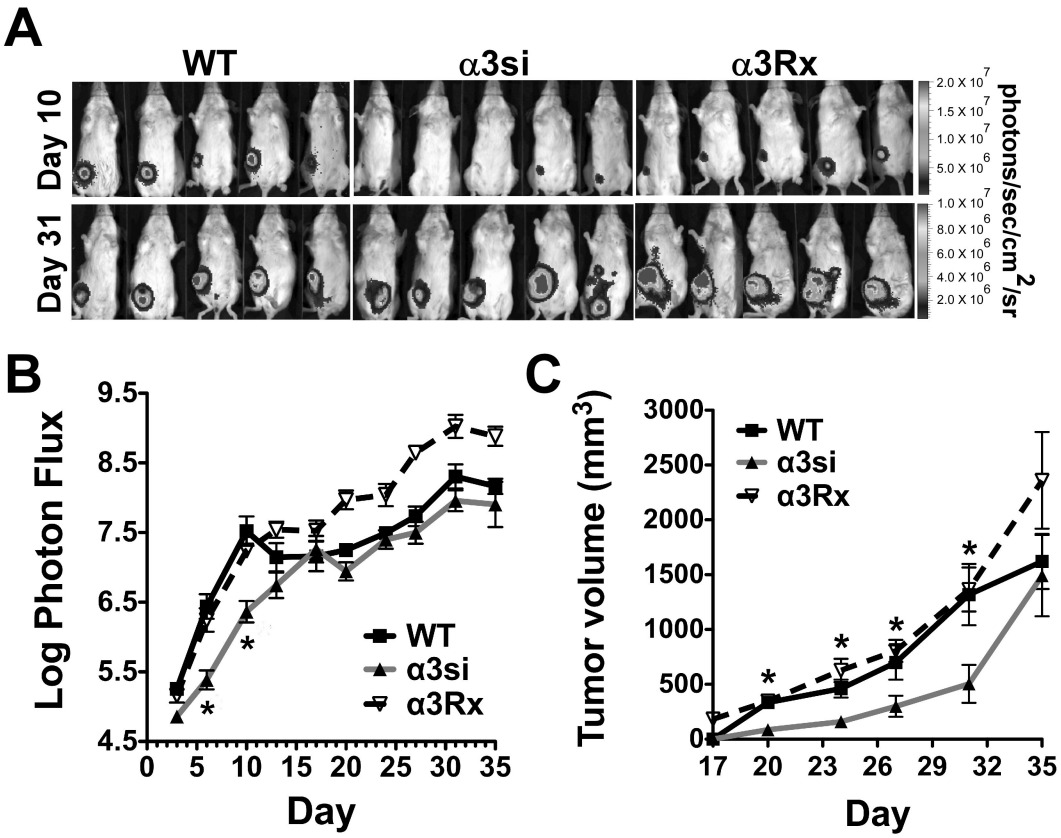

Figure 2. Growth of primary tumors and total tumor burden

On day 0, 5,000 luciferase-expressing 4T1 wild type, α3si, and α3Rx cells were implanted in the 4th mammary fat pad of female Balb/C mice. (**A**) Bioluminescence imaging (BLI) of the cells on day 10 (when α3si tumor cell burden appeared reduced compared to controls) and day 31 (when α3si tumor cell burden appeared similar to wild type). (**B**) Total apparent tumor burden, measured as log photon flux, for the entire timecourse of the experiment. The α3si tumor cell burden was significantly less than wild type or α3Rx on days 6 and 10 (*P<0.001 vs wild type, P<0.01 vs α3Rx, ANOVA with Tukey post-test; n=10 mice per group). The slight reduction in photon flux observed on day 35 was due to the loss of some of the mice with the highest tumor burdens between day 31 and day 35. (**C**) Tumor volumes measured by caliper. The mean volume of the α3si tumors was significantly less than the volumes of both the wild type and α3Rx tumors from day 20 through day 31 (*P<0.01 on day 20, and P<0.05 on days 24-31, ANOVA with Tukey post-test, except for day 27, when α3si was significantly different from α3Rx, but not wild type).

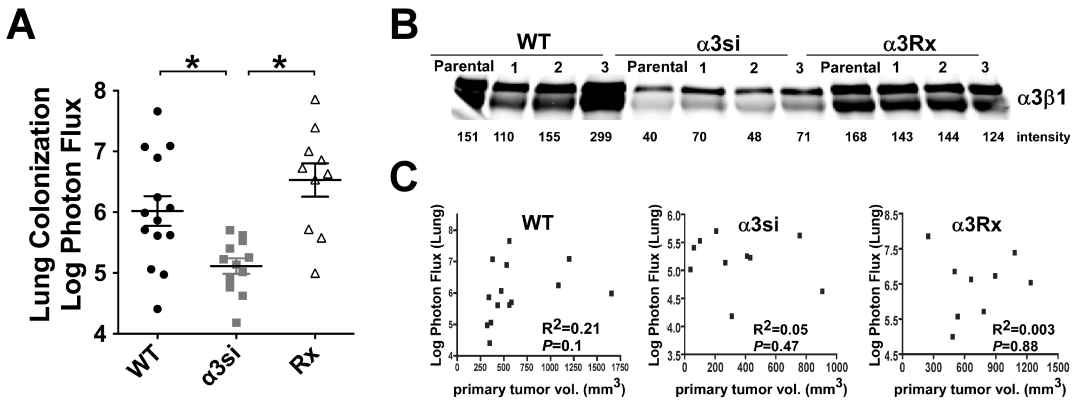

Figure 3. Spontaneous metastasis is significantly impaired in α3 integrin-silenced 4T1 cells

(**A**) Lung colonization as quantified in ex-vivo BLI images (See Figure S4 for representative images). The α3si 4T1 cell colonization was significantly reduced compared to wild type or α3Rx cell colonization (*P<0.05 vs wild type, P<0.001 vs α3Rx, ANOVA with Tukey post-test; n = 10-14 mice per group; bars indicate mean ± SEM). (**B**) Wild type, α3si, and α3Rx 4T1 cells were cell surface-biotinylated, and α3β1 integrin was recovered by immunoprecipitation from Triton X-100 lysates, as in Figure 1. For each set, the lane marked "parental" corresponds to the original cell line implanted into mammary fat pad at the beginning of the assay, and the lanes numbered 1-3 correspond to sublines recovered from lung explants at the end of the assay. Quantification of band intensities by LI-COR blot imager is indicated under each lane (in arbitrary intensity units). (**C**) The relationship between primary tumor volume and lung colonization measured by BLI is graphed for each cell type. Values for R^2 and P from Pearson correlation tests are shown for each graph. In no case was there a significant correlation between primary tumor volume and lung colonization.

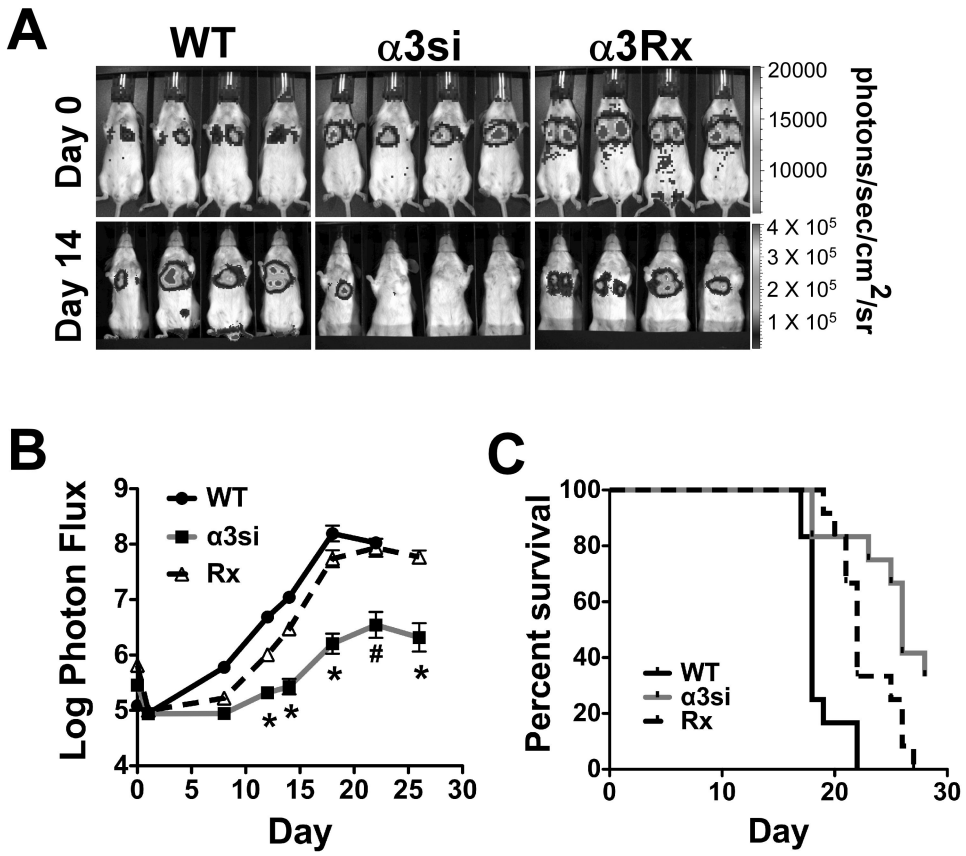

Figure 4. Experimental lung metastasis is significantly impaired in α3 integrin-silenced 4T1 cells

On day 0, 50,000 wild type, α3si, or α3Rx luciferase-expressing 4T1 cells were injected by tail vein into female Balb/C mice. (**A**) BLI imaging on day 0, immediately after tail vein injection and on day 14, about halfway through the assay. (**B**) Total tumor burden (log photon flux) as measured by BLI. Metastatic colonization by the α3si cells was significantly reduced compared to wild type or α3Rx cells from day 12 onward (*P<0.001 vs wild type and α3Rx cells, on days 12-20; #P<0.05 vs wild type and P<0.001 vs α3Rx on day 22; and *P<0.001 vs α3Rx on day 26, ANOVA with Tukey post-test, n=15 mice per group). (**C**) Survival to endpoint for mice bearing wild type, α3si, or α3Rx 4T1 cells. Survival of mice with α3si 4T1 cells was significantly increased compared to mice with wild type or α3Rx 4T1 cells (P<0.0001 vs wild type and P = 0.0127 vs α3Rx, Mantel-Cox log-rank test).

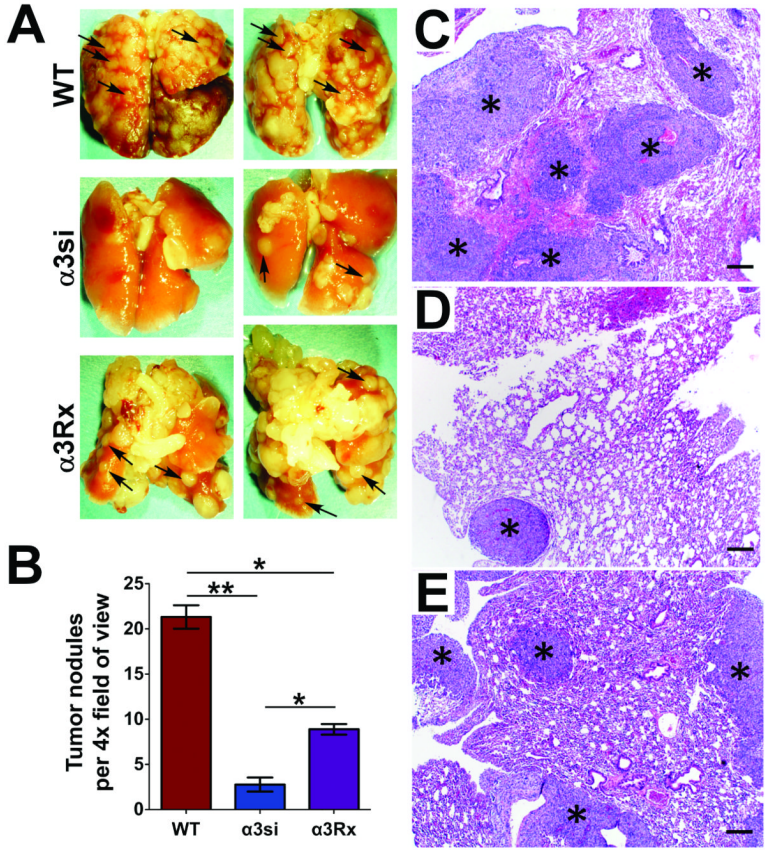

Figure 5. Gross and histologic analysis of experimental lung metastasis

(**A**) Lungs recovered 18-28 days after injection from mice bearing wild type, α3si, or a3Rx 4T1 cells were paraformaldehyde-fixed and photographed using a dissecting microscope prior to paraffin-embedding. Pulmonary metastases appear as pale tan nodules on the surfaces of lungs (arrows point to examples). Fewer nodules were evident on lungs from mice with α3si cells. (**B**) Quantification of tumor nodules per 4X field in H&E-stained sections from paraffin-embedded lungs. The α3si 4T1 cells formed fewer nodules than either wild type or α3Rx 4T1 cells. The wild type cells formed more nodules than the α3Rx cells, indicating a partial restoration of α3 function for the α3Rx cells in this assay. (*P<0.01, ANOVA with Tukey post-test, n=3 mice per group, 3 slides per mouse, 3 fields per slide, for a total of 27 fields per cell type). Shown at right are representative photomicrographs of lungs from mice injected with (**C**) wild type, (**D**) α3si, or (**E**) α3Rx 4T1 cells. Asterisks indicate examples of tumor nodules within the pulmonary parenchyma. HE, bars = 200 μm.

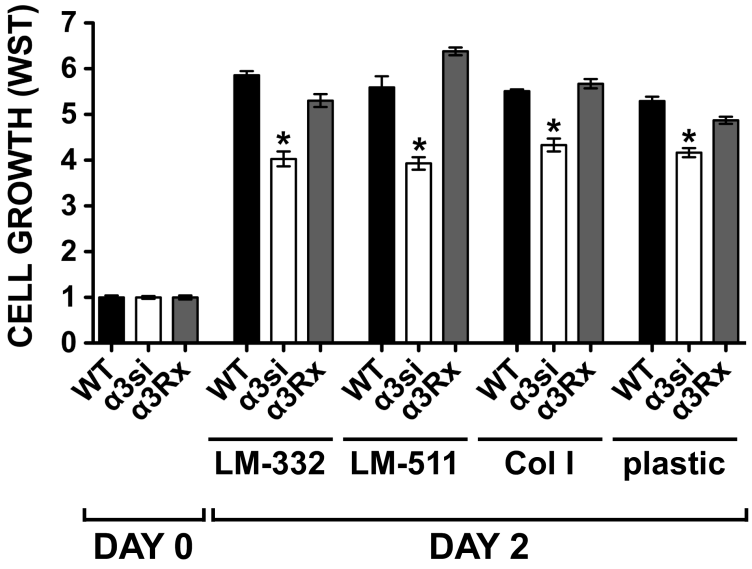

Figure 6. Impaired proliferation of α3-silenced 4T1 cells

Wild type, α3-silenced, and α3Rx 4T1 cells were plated in 2% FBS in wells coated with 1 μg/ml LM-332, 1 μg/ml LM-511, 10 μg/ml collagen I, or in uncoated wells. One set of wells was assayed by WST-1 on day 0 (the day of plating) to measure cells input, and the remaining wells were assayed on day 2. Bars represent mean ± SEM for 6 wells per cell type per condition, normalized to day 0 values. The growth of the α3si cells was significantly less than that of either the wild type or α3Rx cells on all substrates tested (*P<0.001, ANOVA with Tukey post-test).

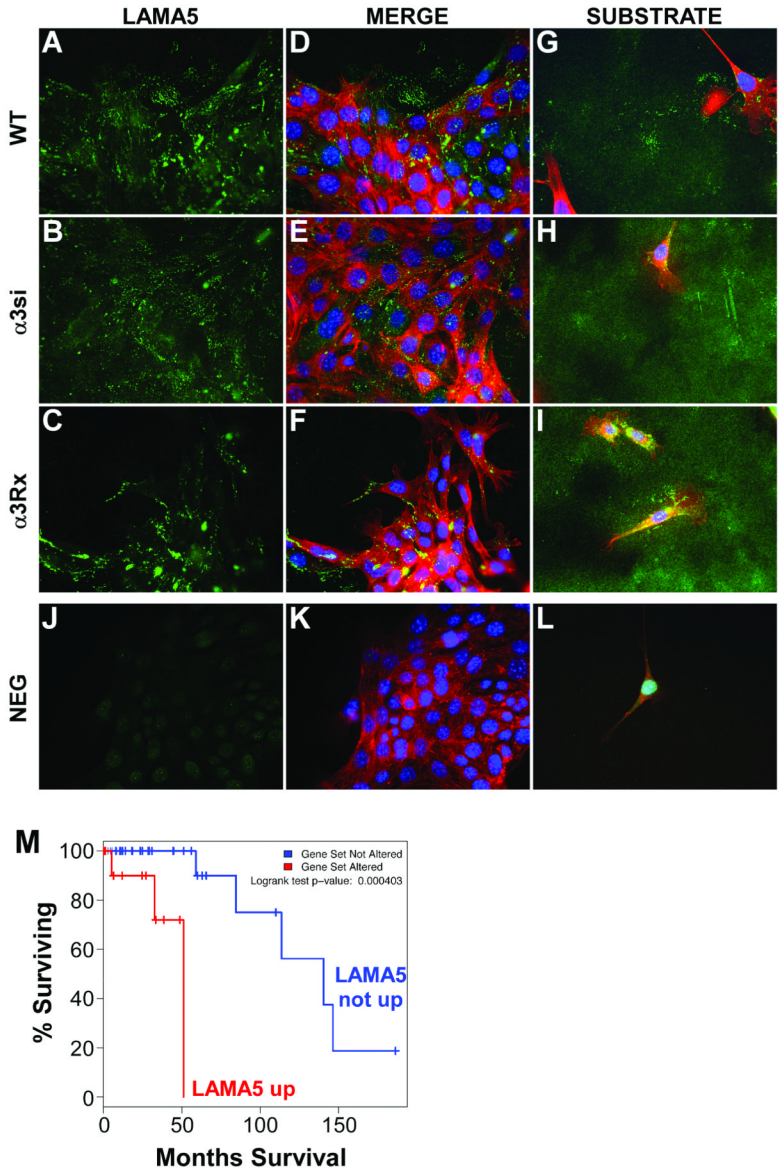

Figure 7. Laminin α5 expression by 4T1 cells

(**A-C**) Wild type, α3si, and α3Rx 4T1 cells were cultured on collagen I-coated coverslips overnight, then fixed and stained with polyclonal anti-laminin α5 antibody (LAMA5). (**D-F**) The merged images show counterstaining for F-actin and nuclei with phalloidin and DAPI. (**G-I**) Longer exposure images in cell-free areas highlight laminin α5 deposition on the substrate. (**J-L**) Negative control staining with normal rabbit IgG. (**M**) Survival analysis of α3 integrin-overexpressing human breast cancer cases, based on whether or not laminin-α5 (LAMA5) is also upregulated. LAMA5 overexpressing cases showed reduced survival (P=0.000403, logrank test).